STAR Protocols

CellPress
OPEN ACCESS

Protocol

Protocol to photoactivate adipose-derived stem cell differentiation using a tightly-focused femtosecond laser

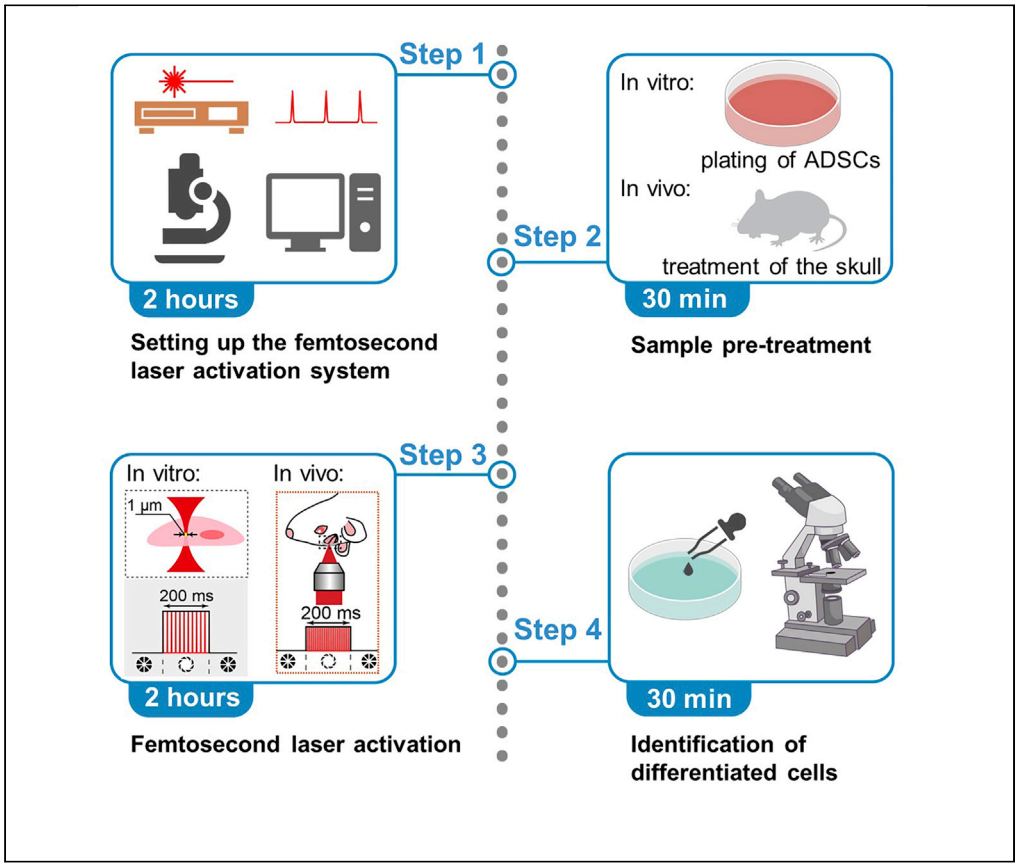

The technology to induce stem cell differentiation is of great importance in life science, stem cell therapy, and regenerative medicine. Here, we detail steps to noninvasively activate stem cell differentiation *in vitro* and *in vivo* using a tightly focused femtosecond laser. We describe how a single-time transient photoactivation can initiate differentiation without any gene engineering, exogenous substances, or physical contact. This protocol enables the differentiation of adipose-derived stem cells to osteoblasts *in vitro* and cerebellar granule neuron progenitors to granule neurons *in vivo*.

Publisher's note: Undertaking any experimental protocol requires adherence to local institutional guidelines for laboratory safety and ethics.

Wanyi Tang, Haipeng Wang, Hao He

tangyixiaowan@sjtu.edu.cn (W.T.)
haohe@sjtu.edu.cn (H.H.)

Highlights

An easy-to-build optical system to provide transient noninvasive photoactivation

All-optical noninvasive approach without exogenous substances or physical contact

Differentiation of several stem cell models *in vitro* and *in vivo*

Tang et al., STAR Protocols *3*, 101574
September 16, 2022 © 2022 The Author(s).
https://doi.org/10.1016/j.xpro.2022.101574

STAR Protocols

CellPress
OPEN ACCESS

Protocol

Protocol to photoactivate adipose-derived stem cell differentiation using a tightly-focused femtosecond laser

Wanyi Tang,[1,2,3,*] Haipeng Wang,[1,2] and Hao He[1,4,*]

[1]School of Biomedical Engineering, Shanghai Jiao Tong University, Shanghai 200030, P.R. China

[2]These authors contributed equally

[3]Technical contact

[4]Lead contact

*Correspondence: tangyixiaowan@sjtu.edu.cn (W.T.), haohe@sjtu.edu.cn (H.H.)
https://doi.org/10.1016/j.xpro.2022.101574

SUMMARY

The technology to induce stem cell differentiation is of great importance in life science, stem cell therapy, and regenerative medicine. Here, we detail steps to noninvasively activate stem cell differentiation *in vitro* and *in vivo* using a tightly focused femtosecond laser. We describe how a single-time transient photoactivation can initiate differentiation without any gene engineering, exogenous substances, or physical contact. This protocol enables the differentiation of adipose-derived stem cells to osteoblasts *in vitro* and cerebellar granule neuron progenitors to granule neurons *in vivo*.

For complete details on the use and execution of this protocol, please refer to Tang et al. (2022).

BEFORE YOU BEGIN

Technologies for stem cell differentiation play an important role in life science research, stem cell therapy and regenerative medicine. Plenty of biochemical technologies for induced differentiation have been developed by using transcription factors (Muffat et al., 2016), small molecule chemical reagents (Burridge et al., 2014), and genetic engineering (Camp et al., 2018). Functional nanomaterials (Chaudhuri et al., 2016), 3D culture (von Erlach et al., 2018), and mechanical stress regulation (Vining and Mooney, 2017) also work for *in vitro* differentiation. These technologies require introduction of exogenous genes, biochemical reagents, or direct physical contact to stem cells. Moreover, the precise delivery of exogenous molecules to target cells/tissues *in vivo* is technically complex. It may raise safety concerns to the *in vivo* applications such as off-target tumorigenic risks (Lee et al., 2013). In this protocol, we present the detailed procedures of our developed optical method to induce *in vitro* and *in vivo* stem-cell differentiation by a femtosecond laser noninvasively, without any gene engineering, biochemical reagents, or other materials.

This protocol provides a detailed description of the optical setup, photoactivation scheme, and experimental procedures for stem-cell differentiation *in vitro* and *in vivo* respectively. This protocol is demonstrated with primary adipose-derived stem cells (ADSCs) and cerebellar granule neuron progenitors (GNPs) from a Math1-GFP; Dcx-DsRed double reporter mouse model. The essential setup includes a femtosecond laser coupled with a confocal microscope. Essential materials for assessment of differentiation results include antibodies for immunofluorescence and potentially toxic biochemicals. Please read the safety data sheets of all relevant experimental materials. Please be aware of all possible hazard risks during the experimental procedures. Before implementing this protocol, users need to be familiar with the optical setup of the microscope system. Please follow the

This is an open access article under the CC BY-NC-ND license (http://creativecommons.org/licenses/by-nc-nd/4.0/).

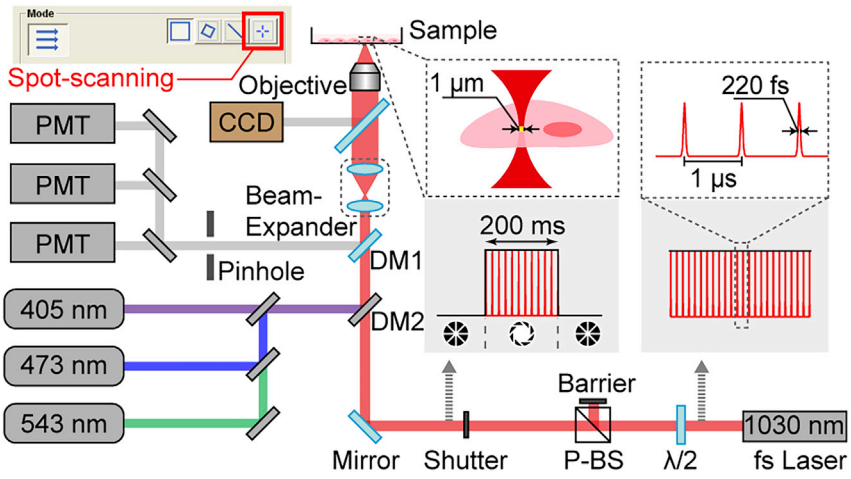

Figure 1. The optical setup of photoactivation by femtosecond laser

The femtosecond laser (1030 nm, ~220 fs, 1 MHz) is focused to a submicron region by a 60 × objective and the duration of the photoactivation is controlled at 200 ms by a mechanical shutter. DM1: a custom-made dichroic mirror with a transmission wavelength of 620–1300 nm (reflection at other visible range). DM2: a custom-made dichroic mirror with a transmission wavelength of 473 nm, 543 nm and 620–1300 nm (reflection at other visible range). λ/2: the half-wave plate. P-BS: polarization beam splitter.

safety instructions of the laser facilities before operating the femtosecond laser source and operate it under the guidance of professionals.

The protocol below describes the specific procedures for initiation of differentiation of rat ADSCs *in vitro* and mouse GNPs *in vivo* by femtosecond-laser photoactivation. This protocol also works for human umbilical cord mesenchymal stem cells (hUC-MSCs) and GNPs *in vitro*. According to the mechanism of this protocol we proposed, the pathways ERK and Wnt/β-catenin initiated simultaneously by Ca^{2+} and weak photodamage mediated the photoactivated differentiation (Tang et al., 2022). Theoretically, this method could be applied to stem cell types that share similar differentiation pathways.

Institutional permissions

All procedures involving animals were approved by the Institutional Animal Care and Use Committee (IACUC) at Shanghai Jiao Tong University and the Ethical Committee of Animal Experiments of School of Biomedical Engineering at Shanghai Jiao Tong University.

Setting up the femtosecond laser activation system

Timing: 1 h

The photoactivation system is established based on a confocal microscope coupling with a femtosecond laser (1030 nm, ~220 fs, 1 MHz) (Figure 1). The femtosecond laser is controlled by a mechanical shutter, collimated to the galvo mirrors in the microscope, and then tightly focused to a submicron region by a water-immersed objective (60 ×, N.A. = 1.2) that simultaneously works for the confocal microscopy. Note a dichroic mirror (transmission: 620–1300 nm) splits the femtosecond laser at 1030 nm and the confocal microscopy at the visible band. The spatiotemporal irradiation of the focused femtosecond laser for photoactivation to the stem cells is controlled by the synchronized galvo mirrors and the shutter. This system enables real-time confocal fluorescence microscopy and simultaneous femtosecond laser activation. The duration of photoactivation is controlled at 100–200 ms by the shutter.

1. Change the dichroic mirrors DM1 and DM2 in the confocal microscope (Figure 1). DM1 is a dichroic mirror (transmission at 620–1300 nm for the coupling of the femtosecond laser, reflection at the other visible range) and DM2 with transmission at 473 nm, 543 nm and 620–1300 nm (reflection at other visible range).

   ⚠ CRITICAL: Check whether the parameters of the DMs can be applied to coupling the near-infrared femtosecond laser. Please note the reset of the dichroic mirrors may influence the range or efficiency of fluorescence collection.

2. Turn on the confocal microscope and femtosecond laser.

   Note: Please keep the power of the femtosecond laser at a low level (less than 50 mW) when preparing the experiments. A half-wave plate (HWP, λ/2) and a polarizing beam splitter is recommended for fine tuning of femtosecond laser power. The ratio of s- and p-polarized components can be continuously tuned by rotating the HWP, thereby finetuning the power of the femtosecond laser.

3. Check the height of the shutter to allow the femtosecond laser beam totally pass through the pinhole of the shutter when it is open.

   ⚠ CRITICAL: Please wear safety goggles properly when operating.

4. The femtosecond laser beam can be guided into the microscope through the hole reserved for the laser source of two-photon microscopy. The dichroic mirrors need to be changed accordingly for the laser coupling and confocal microscopy. Adjust the femtosecond laser beam to the scanning galvanometer and objective of the microscope.

   ⚠ CRITICAL: Keep the laser beam collimated. Check the femtosecond laser beam at the back aperture of the objective. The beam should be collimated and the beam width should match the back aperture of the objective. During the scanning of galvo mirrors, the laser beam should present motionless at the back aperture.

5. The center of field of view (FOV) of the wide-field transmission image from a CCD camera in the microscope should be calibrated with the optical axis of the microscope (see Figure 1). Check if the femtosecond laser is collimated to the objective and focused to the FOV center of the wide-field transmission image of the CCD.

   Note: The colocalization of the center of FOV with the laser focus indicates the coincidence of the femtosecond laser and the optical axis (in theory, they are also coincident with the excitation lasers of the confocal microscope). In principle, if an image frame is defined as a point (one pixel), the femtosecond laser only scans in that single point during the defined photoactivation duration. The defined spot is exactly where the femtosecond laser focus locates and can be labeled in the microscopy images of control software.

6. Start the confocal microscopy software and define a pixel as the spot for photoactivation, usually in the center of the FOV (Figure 1). Define the scanning duration of it as 100–200 ms.

   Note: The spots for photoactivation region can also be defined in other positions and the galvo mirrors can reflect the femtosecond laser there accordingly in a collimated manner.

7. Measure the femtosecond-laser transmission efficiency of the objective with a near-infrared power meter.

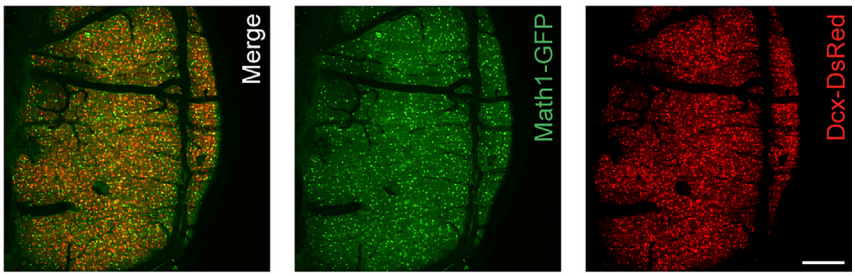

Figure 2. Fluorescence expression characteristics of Math1-GFP; Dcx-DsRed double reporter mouse model
In vivo z-projection of GNPs and GNs in the cerebellum of mice (10 μm/slice, 160 μm in total).

8. Turn off the femtosecond laser source, the confocal microscope and the mechanical shutter until experiments start.

Preparation of Math1-GFP; Dcx-DsRed double reporter mice for *in vivo* photoactivation

Timing: 3 weeks

Math1-GFP; Dcx-DsRed double reporter mouse model can be generated by crossing Math1-GFP mice with Dcx-DsRed mice (Yang et al., 2015). Math1 is a marker of cerebellar GNPs and Dcx is specifically expressed in early differentiated GNs. GNPs (express GFP) and GNs (express DsRed) can be visualized with this animal model by fluorescent microscopy (Figure 2). It is worth noting that cells simultaneously expressing both markers are at an intermediate stage before complete differentiation into GNs.

9. Set up breeding crosses by using one male Math1-GFP mouse with two female Dcx-DsRed mice in each cage.

Note: To ensure the health and population of newborn mice, male mice over 8 weeks old and female mice aged 4–6 weeks for breeding are highly recommended.

10. Genotype the newborn mice using the following primers:

Dcx-DsRed (Forward CCCATGGTCTTCTTCTGCAT; Reverse AAGGTGTACGTGAAGCACCC), Dcx-DsRed Internal Positive Control (Forward: CTAGGCCACAGAATTGAAAGATCT; Reverse GTAGG TGGAAATTCTAGCATCATCC), Math1-GFP (Forward CACATGAAGCAGCACGACTTCT; Reverse AACTCCAGCAGGACCATGTGAT) (Lumpkin et al., 2003). The product lengths are 217 bp, 324 bp and 440 bp in sequence.

Note: PCR Reaction mixture and PCR cycling conditions for genotyping are shown in Tables 1, 2, and 3. See the key resources table for details on primers.

Table 1. PCR reaction master mix

Reagent	Amount
DNA template	1 μL
2 × Taq Buffer	7.5 μL
Primer F	0.5 μL
Primer R	0.5 μL
ddH_2O	6 μL
Total	15.5 μL

Table 2. PCR cycling conditions for Math1-GFP

Steps	Temperature	Time	Cycles
Initial Denaturation	94°C	5 min	1
Denaturation	94°C	30 s	35 cycles
Annealing	55°C	45 s	
Extension	72°C	45 s	
Final extension	72°C	5 min	1
Hold	10°C	Forever	

11. Select double-positive mice for the experiment.

KEY RESOURCES TABLE

REAGENT or RESOURCE	SOURCE	IDENTIFIER
Antibodies		
Rabbit monoclonal anti-Runx2 (Alexa Fluor® 488) (dilution: 1:500)	Abcam	Cat# ab215954; RRID: N/A
Rabbit monoclonal anti-Ki67 (dilution: 1:500)	Abcam	Cat# ab16667; RRID: AB_302459
Rabbit monoclonal anti-Integrin alpha 6 (dilution: 1:500)	Abcam	Cat# ab181551; RRID: N/A
Goat Anti-Rabbit IgG H&L (Alexa Fluor® 488) (dilution: 1:1000)	Abcam	Cat# ab150077; RRID: AB_2630356
Chemicals, peptides, and recombinant proteins		
collagenase type I	Sigma-Aldrich	Cat# C0130
BASIC MEM alpha culture medium	Gibco	Cat# C12571500BT
Fetal Bovine Serum	Gibco	Cat# 10270-106
Penicillin-Streptomycin (10,000 U/mL)	Gibco	Cat# 15140122
Trypsin-EDTA (0.25%), phenol red	Gibco	Cat# 25200056
PBS	Gibco	Cat# C10100500BT
Dexamethasone	Sigma-Aldrich	Cat# D4902
β-glycerophosphate	Sigma-Aldrich	Cat# G9422
L-Ascorbic acid-2-phosphate	Sigma-Aldrich	Cat# A8960
Alizarin Red S	Sigma-Aldrich	Cat# A5533
4% paraformaldehyde	Beyotime Biotechnology	Cat# P0099
10% Triton X-100 solution	Shanghai Yuanye Bio-Technology Co., Ltd	Cat# R21412
skim milk powder	Sangon Biotech	Cat# A600669
Tween-20	Sangon Biotech	Cat# A100777
Experimental models: Organisms/strains		
Mouse: C57BL/6J-Tg (Dcx-DsRed) 14Qlu/J (male mice over 8 weeks old, female mice aged 4–6 weeks)	The Jackson Laboratory	JAX: 009655
Mouse: Math1-GFP (male mice over 8 weeks old, female mice aged 4–6 weeks)	Lumpkin et al. (2003) Novartis	N/A
Math1-GFP; Dcx-DsRed double reporter mouse (20–25 days old, male mice for in vivo photoactivation)	By crossing Math1-GFP mice with Dcx-DsRed mice	N/A
SD Rat (7-day postnatal, male rats for isolation of primary ADSCs)	Shanghai Laboratory Animal Center	N/A
Oligonucleotides		
Primer: Dcx-DsRed Forward: CCCATGGTCTTCTTCTGCAT	The Jackson Laboratory	N/A
Primer: Dcx-DsRed Reverse: AAGGTGTACGTGAAGCACCC	The Jackson Laboratory	N/A
Primer: Dcx-DsRed Internal Positive Forward:CTAGGCCACAGAATTGAAAGATCT	The Jackson Laboratory	N/A

(*Continued on next page*)

Continued		
REAGENT or RESOURCE	SOURCE	IDENTIFIER
Primer: Dcx-DsRed Internal Positive Reverse: GTAGGTGGAAATTCTAGCATCATCC	The Jackson Laboratory	N/A
Primer: Math1-GFP Forward: CACATGAAG-CAGCACGACTTCT	Lumpkin et al. (2003)	N/A
Primer: Math1-GFP Reverse: AACTCCAG-CAGGACCATGTGAT	Lumpkin et al. (2003)	N/A
Recombinant DNA		
Plasmid: pCMV R-CEPIA1er	Addgene	#58216
Plasmid: pCMV G-CEPIA1er	Addgene	#58215
Software and algorithms		
ImageJ	NIH	https://imagej.nih.gov/ij/index.html
GraphPad Prism.7.00	GraphPad Software	https://www.graphpad.com/scientific-software/prism/
FLUOVIEW Viewer	Olympus	https://www.olympus-lifescience.com.cn/en/support/downloads/
Other		
Glass bottom cell culture dish	NEST	Cat# 801001
Femtosecond laser	Menlo Systems	BlueCut
Confocal microscope	Olympus	FV1200
60 × objective (N.A. = 1.2)	Olympus	UPlanSApo
Mechanical shutter	Daheng Optics	GCI-73M/GCI-7101M
Half-wave plate	Thorlabs	WPH10M-1030
Polarization beam splitter	Daheng Optics	GCC-402122

MATERIALS AND EQUIPMENT

Culture medium for ADSCs		
Reagent	Final concentration	Amount
BASIC MEM alpha culture medium (MEM-α)	89%	449 mL
Fetal bovine serum (FBS)	10%	50 mL
Penicillin-Streptomycin (10,000 U/mL)	1%	1 mL
Total	**100%**	**500 mL**
The prepared culture medium for ADSCs can be stored at 4°C for 3 months.		

Dexamethasone osteogenic differentiation medium (DEX)		
Reagent	Final concentration	Amount
Dexamethasone (100 μM)	10 nM	10 μL
β-glycerophosphate	10 mM	216.04 mg
L-Ascorbic acid-2-phosphate	50 μM	1.45 mg
Culture medium for ADSCs	n/a	Up to 100mL
Total	**n/a**	**100 mL**
The prepared DEX medium can be stored at 4°C for 3 months.		

STEP-BY-STEP METHOD DETAILS

Isolation and culture of primary ADSCs

Timing: 3 h

Our protocol is a streamlined adaptation from previously established protocols (Estes et al., 2010). Primary ADSCs is used as a viability demonstration of this protocol. If ADSCs or other stem cells are already available, skip directly to step 14.

Table 3. PCR cycling conditions for Dcx-DsRed

Steps	Temperature	Time	Cycles
Initial Denaturation	94°C	2 min	1
Denaturation	94°C	20 s	10 cycles
Annealing	65°C	15 s	
Extension	68°C	10 s	
Denaturation	94°C	15 s	28 cycles
Annealing	60°C	15 s	
Extension	72°C	10 s	
Final extension	72°C	2 min	1
Hold	10°C	Forever	

1. Sterilize the surgery tools and operation area.
2. Prepare the culture medium for ADSCs: BASIC MEM alpha culture medium (MEM-α) with 10% fetal bovine serum (FBS) and 1% Penicillin-Streptomycin (10,000 U/mL). See materials and equipment.
3. Euthanize 7-day postnatal male SD rats using methods approved by the animal welfare committee.

   Note: About 10^7 ADSCs can be extracted from the adipose tissue of 5 rats.

4. Spray the surface of the rats with 75% ethanol and place them in the operation area.
5. Dissect tlistbhe adipose tissue of the groin and epididymal/parametrial fat pads.
6. Wash the adipose tissue in PBS buffer and mince them with a sterilized scissor.

   Note: It is best to cut the tissue into evenly sized pieces for better control of digestion time.

7. Transfer the tissue to a 15 mL tube. Mix it in the ratio of 1:1 (vol/vol) with 2% collagenase type I solution for digestion. Incubate for 30–60 min at 37°C until few tissue clumps are visible.

   Note: Gently agitate the tube every 8–10 min for better mix during digesting. Here you can directly use the incubator shaker instead of manual operation.

8. Add 2 mL digestive termination buffer (culture medium) to the tube, and dissociate the cells by gently pipetting up and down.
9. Centrifuge it at 300 × *g* for 5 min at room temperature (25°C).
10. Discard the supernatant containing adipocytes and debris and resuspend the cell pellets in 7 mL culture medium.
11. Filter the cell resuspension through a 70-μm cell strainer to obtain single-cell suspension of ADSCs.
12. Seed the single cells at 1 × 10^6/mL into 100-mm culture dishes and initially incubate for 72 h at 37°C and 5% CO_2.
13. Passage the cells or refresh the medium every 2 days.
    a. Passage every 2 days during normal culture and expansion.
    b. Refresh the medium every 2 days after photoactivation for up to 21 days.

Plating of ADSCs for *in vitro* photoactivation

Timing: 30 min

The femtosecond laser successively activates individual stem cells. Thus, the time for the entire experiment is dependent on the throughput of cells for photoactivation. Therefore, a large

amount of ADSCs is quite time-consuming. But too few cells may lead to poor cell growth in subsequent culture. Therefore, the appropriate plating conditions (cell density and total cells) are important in this protocol. In this protocol, initially 1500 cells in a dish is recommended. The part below describes the specific steps of preparing rat ADSCs for photoactivation *in vitro*. If other types of stem cells are used, the processing time of each step may need to be adjusted accordingly.

14. At cell confluency of 80%, take out the dishes for passaging and plating.
15. Wash the cells with pre-warmed PBS buffer 3 times.
16. Add 1 mL of 0.25% Trypsin-EDTA for 30 s to digest the ADSCs and then 2 mL of culture medium to terminate it. Transfer the cell resuspension to a new 15-mL tube.
17. Centrifuge the tube at 300 × *g* for 5 min at room temperature (25°C).
18. Discard the supernatant and resuspend the cell pellets in culture medium to obtain 3×10^5/mL cell suspension.
19. Carefully drop 5 μL cell suspension at the center of a petri dish with 15-mm glass bottom. The cell number is around 1500 in the dish.

⚠ CRITICAL: After dropping 5 μL cell suspension, take special care to prevent the droplet from any movement, to present a clear edge of the cell growth region (Figure 3A). All commercial tissue culture (TC) treated glass-bottom petri dishes can work for good adherence of cells. In our experiments, NEST® confocal dishes (Cat. No.: 801002) were used. The adhesion duration of cells was provided here accordingly. If dishes of other brands are used, there might be some variation of adhesion time of cells. Some pre-tests might be needed to explore the cell adherence. See problem 1.

20. Place the dish in the incubator for 2 h at 37°C and 5% CO_2 and wait for the cells to adhere to the bottom.
21. Add another 2 mL culture medium and incubate it for 24 h before photoactivation.

Note: The supplement of culture medium here should be particularly gentle to prevent poorly adherent cells from being washed away.

In vitro photoactivation

Timing: 2 h

The following steps apply to the photoactivation of stem cells *in vitro*.

22. Turn on the femtosecond laser source, the confocal microscope and the mechanical shutter. Ensure the shutter is closed. Set the power of femtosecond laser (1030 nm, ~220 fs, 1 MHz) at 10–15 mW at the specimen.

Note: It is usually necessary to turn on the laser for more than half an hour before the experiment to warm up the laser system for the stability of output power. The Laser power needs to be measured with a power meter. See problem 3.

23. Set the excitation laser at 543 nm at 0.5 mW for transmission bright-field microscopy.

Note: There is no need to set the laser to high power because the morphology of cells can be observed with extremely low excitation power by the confocal transmission bright-field microscopy.

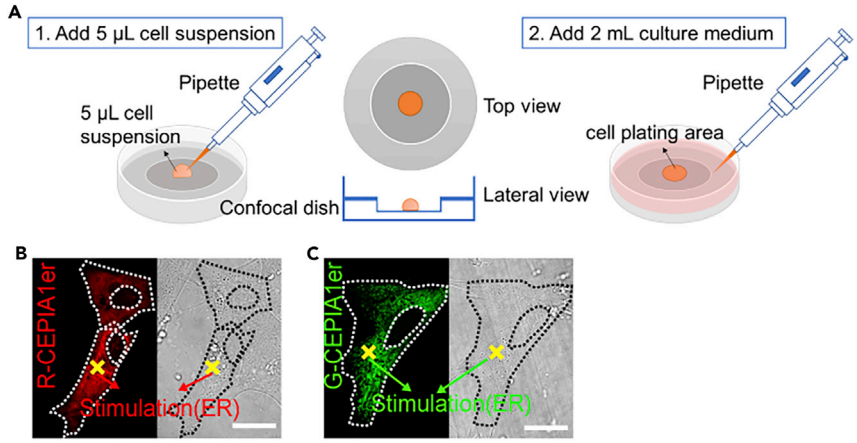

Figure 3. Preparation of photoactivation experiments

(A) Schematic of cell plating.

(B) Fluorescence and brightfield images of ADSCs transfected with R-CEPIA1er and G-CEPIA1er (two ER-expressed fluorescent proteins) plasmids. The focus of femtosecond laser is located in endoplasmic reticulum (ER) region. Arrows: the laser activation region. Scale bar, 20 μm. This figure was reused from Tang et al. (2022).

24. Set imaging parameter at 800 × 800 pixels, 2.0 μs/pixel (the pixels of each image can be set according to practical imaging preference which should present clear cell images at least). Set the correction collar of the objective at 0.17 (μm).

⚠ CRITICAL: Check the thickness of the glass bottom of the dishes. The correction collar of the objective must match the penetration depth of microscope images through the glass slide. It is important to set it correctly before imaging. If the thickness of glass slide is not 0.17 mm, change the correction collar of the objective accordingly.

25. Put the dish with ADSCs on the microscope stage. Tune the objective (60 ×, N.A. = 1.2) vertically to acquire clear bright-field confocal images of cells by the transmission channel.

⚠ CRITICAL: Be sure to use an objective with a high numerical aperture (> 1.0) to obtain the tightly-focused femtosecond laser to confine the thermal effect in the focal volume and obtain the high photon density for multiphoton excitation. There is no need to change the medium before the laser activation experiment.

26. Switch to the point-scanning mode and position the laser focus in the region of endoplasmic reticulum (ER) (cytoplasm near the nucleus) in the target cell. See Figure 3B.

Note: Keep the imaging focal plane at the position where the cell topography is clearest in the brightfield image. Empirically, this imaging plane (the objective position at the z-axis) allows the femtosecond laser focused inside the cell in the z direction (vertically in the ER) if the femtosecond laser is strictly collimated. The laser focus should not locate in the edge of cells to prevent the laser focus from staying outside vertically.

⚠ CRITICAL: A calibration between the focus of femtosecond laser and the imaging plane of the transmission bright-field microscopy (confocal fluorescent microscopy) is highly recommended before experiments here. A 3D standard sample for fluorescent microscopy can be imaged by the femtosecond laser (two-photon microscopy) and transmission bright-field microscopy respectively. Tune the objective to get exactly the same images. Record the tuning distance of objective to acquire the image.

27. Pre-set the opening gate of the mechanical shutter as 200 ms for a single time (10–15 mW at specimen).
28. Start the point-scanning and simultaneously open the mechanical shutter as a single-time 200 ms photoactivation to the target cells.
29. Move the scan point to the next cell, localize the laser focus to the ER region, and repeat step 28 until all cells in the FOV are photoactivated.
30. Move the microscope stage to get the image of the next neighboring FOV.
31. Repeat step 28–30 until all cells in the entire dish are activated.

Note: The cells may deteriorate during photoactivation experiments (steps 25–31). See problem 2.

32. Change the medium half an hour after the photoactivation experiment. Culture the cells and change the cell medium every 2 days up to the 21st day after photoactivation.

Note: For the classic drug-induced osteogenic differentiation of ADSCs, it takes about 21 days to complete the differentiation. Here, we perform the Alizarin Red assay on Day 21 and compared the results with dexamethasone-induced osteogenic differentiation. For other types of stem cells, the date of differentiation test can be adjusted accordingly.

Identification of differentiated cells

Timing: 30 min

Here we describe the procedures for immunofluorescence microscopy and Alizarin Red S staining to access the differentiated osteoblasts (Figure 4). In this protocol, we take Runx2 as an example.

Note: To exclude false-positive signals, both negative and positive controls are required for Alizarin Red staining. ADSCs cultured with dexamethasone osteogenic differentiation medium (DEX) (10 nM dexamethasone, 10 mM β-glycerophosphate, 50 μM L-Ascorbic acid-2-phosphate and 10% FBS in culture medium) is set as a positive control. For more information on the materials, see the key resources table. There are several reasons for a low percentage of differentiated cells. See problem 4.

33. Immunolabeling of Runx2 on Day 7
    a. Take out the dishes plated with the photoactivated ADSCs from the incubator. Wash each dish with 1 mL pre-warmed PBS 3 times.

    Note: Pre-warm the PBS to prevent cells from adhering loosely.

    b. Fix the cells with 2 mL pre-warmed 4% paraformaldehyde (PFA) for 15 min.
    c. Wash cells for 3 × 5 min in PBST (PBS with 0.1% Tween 20).
    d. Treat the cells with 2 mL PBST containing 0.1% Triton X-100 for 15 min.
    e. Wash cells for 3 × 5 min in PBST.
    f. Block non-specific adsorption of proteins with 2 mL 5% skim milk in PBST at room temperature (25°C) for 1 h and wash cells in PBST for 3 min.
    g. Incubate the cells with 2 mL solution of Runx2 primary antibody (1:500 in PBST, rabbit, conjugated with Alexa Fluor® 488) at 4°C overnight (12–16 h).
    h. Wash each dish for 3 × 5 min in PBST.
    i. Capture the images by confocal microscopy (excited by 473 or 488 nm laser).
34. Alizarin red S staining on Day 21

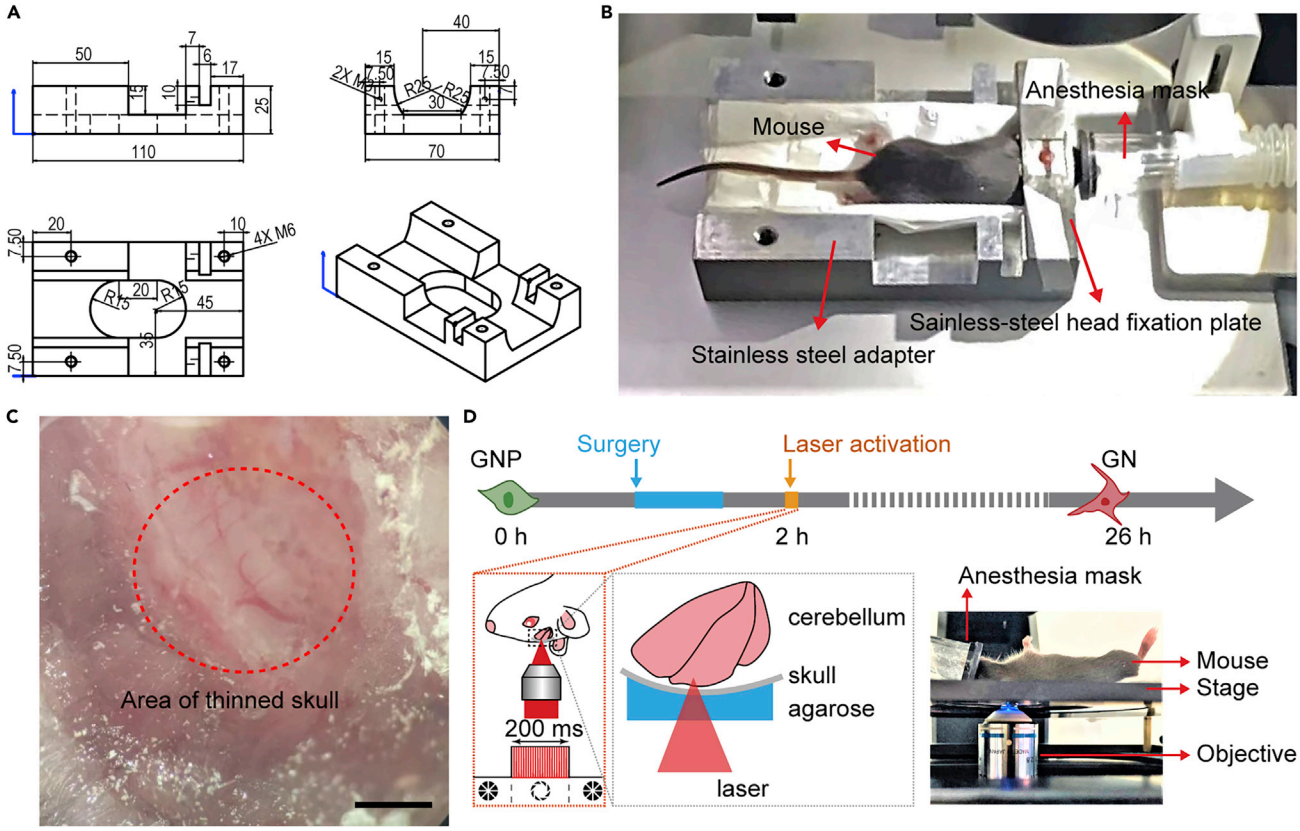

Figure 4. Imaging and laser-activated differentiation of GNPs to GNs *in vivo*

(A) The design drawing of the custom stainless-steel mouse adapter.

(B) Mice are secured to the adapter.

(C) The blood vessels under the thinned skull become visible. Scale bar, 2 mm.

(D) The experimental design for photoactivation of GNPs *in vivo*. Surgery: pre-treatment before photoactivation. Insert: the mice on the stage with anesthesia during the photoactivation experiment. This figure was reused from Tang et al. (2022).

a. Prepare Alizarin Red S solution: add 1 *g* of alizarin red S powder to 50 mL of ddH_2O, tune the pH value of the mixture to 4.2 with 10% NH_4OH, and filter the solution through a 0.22 μm strainer.

Note: The prepared Alizarin Red S solution can be stored at 4°C for 1 month in the dark.

b. Take out the dishes plated with the photoactivated ADSCs from the incubator. Wash the cells with 1 mL pre-warmed PBS 3 times.
c. Fix the cells with pre-warmed 2 mL 4% paraformaldehyde (PFA) for 30 min.
d. Wash each dish for 3 × 5 min in 1 mL ddH2O.
e. Treat cells with 2 mL Alizarin Red S solution for 3 min.
f. Wash each dish for 3 × 5 min in 1 mL ddH2O.
g. Capture the images by bright-field microscope.

Pre-treatment of mice for *in vivo* photoactivation

Timing: 30 min

For better *in vivo* imaging and photoactivation of GNPs in the cerebellum, the Math1-GFP; Dcx-DsRed mice are pre-treated before photoactivation. The opaque skull of the mouse is an

insurmountable obstacle for deep microscopy. Its thick and uneven internal structure causes extremely large scattering and complex distortion, making it difficult to observe neurons beneath the skull. To overcome this problem, surgery is usually required to thin the skull or establish a localized cranial window for long-term observation. In this protocol, to protect the intact cerebellum from any possible damage of craniotomy, thinning the skull is recommended (Figure 4).

35. Anesthetize the Math1-GFP; Dcx-DsRed double reporter mouse (20–25 days old, male) with isoflurane (1–2%) in 0.5–1.0 L/min of O_2 during surgery. Many GNPs become mature at P21 while there remained quite a few undifferentiated GNPs.

Note: If this transgenic mouse model is not preferred, any fluorescent dyes to label neurons can be used for visualization of neural stem cells/GNPs in the cerebellum.

36. Hold the mouse on a custom stainless steel mouse adapter as shown in Figure 4A. Apply eye ointment to prevent mouse eyes from drying out.
37. Wipe the skin above the cerebellum with iodophor. Remove the hair and skin above the cerebellum with sterilized ophthalmic scissors. Use a scalpel to scrape the periosteum from the skull and carefully remove the muscles overlying the cerebellum.
38. Wipe the surface of the skull with saline mixed with penicillin.

⚠ CRITICAL: This step aims to eliminate any inflammation. See problem 5.

39. Slightly thin the localized skull (about 2.0 mm caudal to lambda). Grind the skull very gently with a 0.5mm cranial drill until the underlying blood vessels are visible.

⚠ CRITICAL: Use a cranial drill to remove the topmost bone and then the bone trabecula in the middle layer of the skull, and finally grind the lowest layer of bone until the skull deforms with a light touch. The thin-skull surgery has developed into a relatively mature operation procedure, and many protocols and videos have been reported (Marker et al., 2010; Yu and Zuo, 2014). Be careful not to drill through the skull. Ideally, the blood vessels under the skull are clearly visible when the skull is maximally thinned, while the integrity of the skull is still maintained (Figure 4C). Do not injure the blood vessels below the skull. Do not perforate or crack the skull.

40. Once the skull is dry, glue the custom stainless-steel head fixation plate (as shown in Figure 4B) to the skull anterior from the lambda with dental cement.
41. After the dental cement dries, fix the stainless-steel plate to one end of the mouse adapter with medical tape.
42. Keep the mouse anesthetized before and during microscopy and photoactivation experiments.

In vivo photoactivation

Timing: 2 h

43. Turn on the femtosecond laser source, the confocal microscope and the mechanical shutter. Ensure the shutter is closed. Set the excitation lasers at 473 nm and 543 nm at 0.5 and 0.8 mW respectively. Set the power of femtosecond laser (1030 nm, ~220 fs, 1 MHz) at 5 mW at the cerebellum.
44. Place the pre-treated mouse on the microscope stage. Move the stage to put the cerebellum under the objective if the microscope is upright. Tune the water-immersed objective (60 ×, N.A. = 1.0) closely to the skull to allow the water on it to contact with the skull.

Note: If the microscope is inverted, lay the mouse on the back on the stage and move the cerebellum to the objective. In this protocol, we take the inverted microscope as an example.

45. Run the fast-scanning mode of the confocal microscope, and tune the objective vertically to acquire a clear fluorescent image of the neurons in the cerebellum (Figure 4D). The GNPs are indicated by the green fluorescence of Math1-GFP and GNs by the red fluorescence of Dcx-DsRed.

Note: The number of GNPs is closely related to the age of the mice. Generally, GNPs decrease as the mouse age. At different microscopy depths, different proportions of GNPs and GNs can be observed. GNPs account for the largest proportion at the surface layer. In the deep cerebellum, GNPs decrease but GNs increase. In young mice, GNPs form dense layers with distinct morphological characteristics near the surface. A single layer or the whole cerebellum can be selected for photoactivation.

46. Activate the GNPs in FOV one by one by femtosecond laser at 5–10 mW for 200 ms with the same steps in steps 28–31.

Note: The femtosecond laser power should match the depth of different GNPs. It is difficult here since the cerebellum tissue attenuates the laser greatly along with penetration depth due to the tissue scattering and absorption. The exact laser power inside the cerebellum tissue cannot be measured directly. Some simulation results of laser penetration efficiency in brain tissue can be referenced to estimate the laser power inside. Experientially, at 50 μm below the skull, the required photoactivation power is about 5 mW at the skull; at 150 μm below the skull, the required power is about 7 mW.

47. GNPs in another region in the plane or at different depths can be activated subsequently.

Note: When performing photoactivation experiments, carefully record the location of stimulated cells based on vessel and depth information, such that the same area can be re-localized again for observation at some time after photoactivation.

48. Re-localize the photoactivation region in steps 44–47. Re-observe and count GNs (red) and GNPs (green) in the photoactivated region in the cerebellum after 24 h. See problem 5.

Note: The differentiation of GNPs into GNs can be observed after 24 h of photoactivation. The differentiation can also be observed later. Please note after longer time, the recovery and growth of the skull exacerbate the difficulty of re-localizing the photoactivated regions.

EXPECTED OUTCOMES

For photoactivated differentiation *in vitro*, a tightly-focused femtosecond laser is used to provide a single-time transient activation to ADSCs. Each ADSC suffers only 200-ms laser irradiation in a localized submicron region (which is colocalized with the laser focus) in ER. Under the conditions in this protocol, the osteogenic differentiation marker Runx2 presents higher expression than it of the control group 7 days after photoactivation (Figure 5A). Numerous cells are alizarin red S positive, significantly more than it of control 21 days after photoactivation (Figure 5B), indicating the osteogenic differentiation. This technique is also applicable to cultured hUC-MSCs (Figure 6A) and cultured GNPs (Figure 6B) *in vitro*. This protocol was further applied to photoactivation on human airway basal stem cells (BCs). An increase in the expression of the cell proliferation marker Ki67 was found 24 h after photoactivation (Figure 6C). The differentiation of those photoactivated BCs to club cells could be finally induced in the in vivo in the damaged airway environment. The mechanism of this protocol is, as we proposed, the pathways ERK and Wnt/β-catenin initiated simultaneously by Ca^{2+} and weak photodamage elicit the laser-induced differentiation (Tang et al., 2022). It could

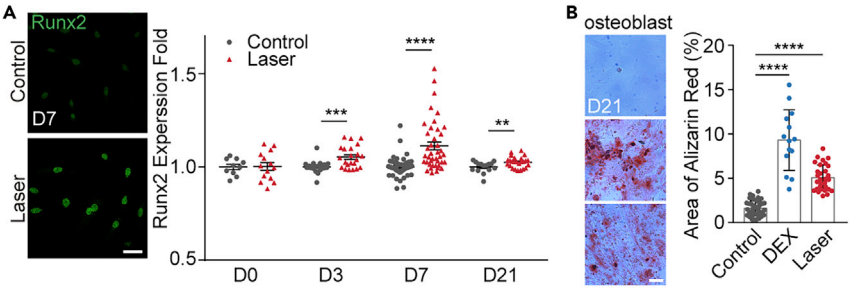

Figure 5. Femtosecond laser induced differentiation of ADSCs into osteoblasts

(A) The immunofluorescence microscopy images of Runx2 in ADSCs after laser activation on Day 3 (n=22 fields in 7 independent trials), Day 7 (n=41 fields in 14 independent trials), and Day 21 (n=25 fields in 8 independent trials). Right panel: the quantified Runx2 level.

(B) The positive ratio of area staining with Alizarin Red S in the differentiated cells on Day 21 induced by dexamethasone (DEX, 10 nM), Laser (1030-nm laser at mode M (0.2 s) respectively (Control, n=41 fields in 11 independent trials; DEX, n=14 fields of view in 5 independent trials; Laser-1030 nm/0.2 s, n=31 fields in 9 independent trials). Graphs include all data points and mean ± SEM. The significance is calculated using unpaired student's t-test (indicated with stars). * $p < 0.05$, ** $p < 0.01$, *** $p < 0.001$. Scale bar, 20 μm. This figure was reused from Tang et al. (2022).

be expected this method could probably work on differentiation of various types of stem cells if their differentiation is related to these two pathways. However, to induce differentiation of other stem cell types, this method could probably work, but the photoactivation parameters should be adjusted accordingly.

For *in vivo* differentiation induction, the differentiation of GNPs to GNs in the cerebellum of live mice can be initiated solely by transient photoactivation. A significant increase in the proportion of differentiated GNs should be observed 24 h after photoactivation (Figure 7).

QUANTIFICATION AND STATISTICAL ANALYSIS

All images were processed by ImageJ (free download from NIH). Quantitative data are presented as the means ± the standard error of the mean (SEM) from at least 3 independent experiments. Statistical analysis and graphs were conducted with GraphPad Prism 7.0 software, while student's t-test and paired t-test were applied when appropriate. In all cases, significance is stated as follows: * $p < 0.05$, ** $p < 0.01$, *** $p < 0.001$; **** $p < 0.0001$, confidence intervals of 95%.

LIMITATIONS

The above protocol induces stem cell differentiation by femtosecond photoactivation *in vitro* and *in vivo*.

Although this method has been demonstrated with the differentiation of ADSCs and hUC-MSCs in vitro, and GNPs to GNs in vitro and in vivo, the universality of it needs further to be investigated. If the differentiation of some stem cells is totally not related to ERK, Wnt, or Ca^{2+}, this method could hardly work.

The throughput of this technology is greatly limited by the single-cell activation scheme. For each cell, the location of photoactivation needs to be manually defined to the appropriate location inside the cell. The throughput of this method can achieve around only 500–1000 cells/h. A potential solution is programming the system to work automatically by analyzing images and selecting cells with machine learning and controlling the laser to activate each cell.

The *in vivo* photoactivation in the cerebellum is greatly limited by the penetration depth of the laser, which is a classic challenge to all-optical microscopy *in vivo*. The effective depth of photoactivation

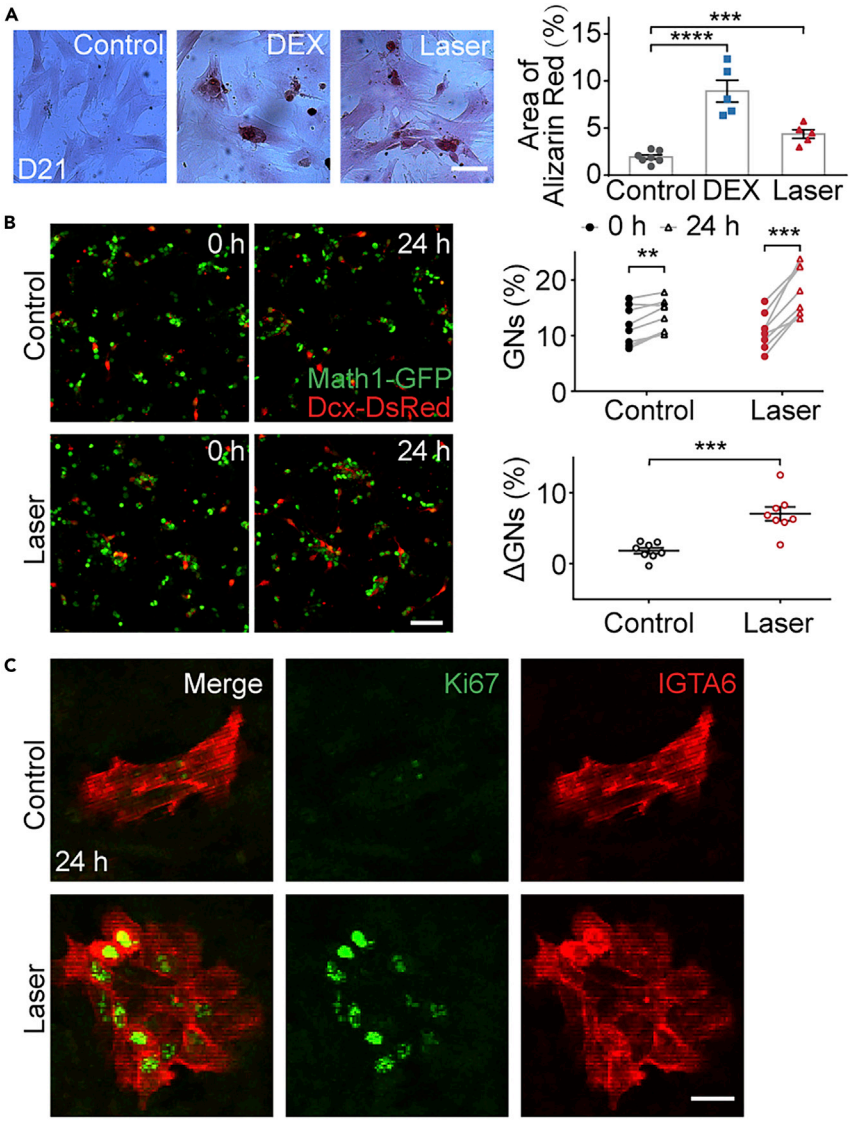

Figure 6. Femtosecond laser induced differentiation of hUC-MSCs and GNPs and proliferation of BCs *in vitro*

(A) The differentiation of hUC-MSCs to osteoblasts activated by the laser *in vitro* indicated by Alizarin Red S staining (n=5 fields of view in 3 independent trials). Scale bar, 20 μm.

(B) The laser-induced differentiation of GNPs to GNs *in vitro* 24 h after photoactivation. Right-upper: the ratio of differentiated GNs before and 24 h after laser activation. Right-lower: the change ratio of GNs. n=8 fields of view in 3 independent trials in the control and the laser activation group. Scale bar, 50 μm.

(C) The enhanced proliferation of human airway basal stem cells (BCs) induced by femtosecond laser 24 h after photoactivation indicated by immunofluorescence of Ki67. Integrin alpha 6 (IGTA6) is a specific protein expressed by BCs. Scale bar, 20 μm. Graphs include all data points and mean ± SEM. The significance is calculated using unpaired student's t-test in (A) and (B) lower while paired t-test in (B) upper (indicated with stars). * $p < 0.05$, ** $p < 0.01$, *** $p < 0.001$; **** $p < 0.0001$. The Figure (A) and (B) was reused from Tang et al. (2022).

by the femtosecond laser at 1030 nm cannot exceed 1 mm. Scattering and absorption by the cerebellum tissue hinder the penetration of laser. Currently, this technique can only be applied to photoactivation of stem cells in superficial tissues (e.g., cerebellar GNPs).

TROUBLESHOOTING

Problem 1

Bad adherence of the seeding cells in confocal dishes (steps 19–21).

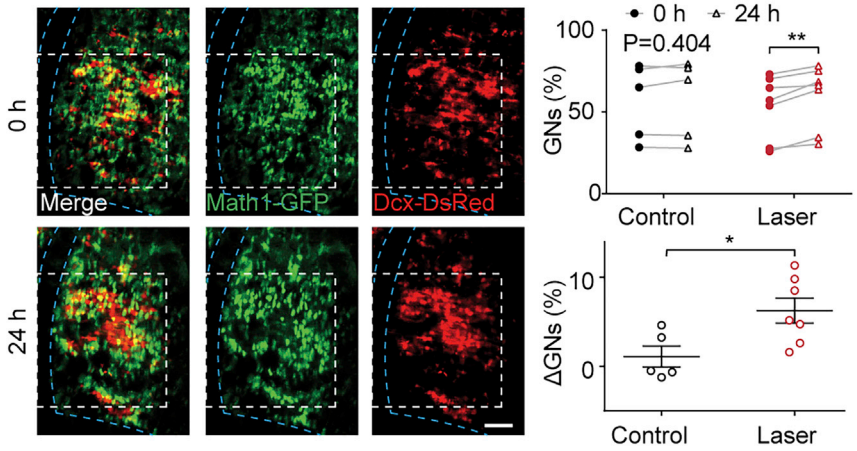

Figure 7. Femtosecond laser induced differentiation of GNPs into GNs 24 h after photoactivation

Left: GNPs (green) and GNs (red) at 100–200 μm depth. Right-upper: the ratio of differentiated GNs in those two groups. Right-lower: the change ratio of GNs before and 24 h after laser activation in those two groups respectively. Dashed blue line: a blood vessel. Boxes with the white dashed line: the area where GNPs inside were activated by laser. n=5 fields in control and 7 fields in the laser activation group in 5 mouse cerebellums. Scale bar, 50 μm. Graphs include all data points and mean ± SEM. The significance is calculated using unpaired student's t-test in the lower graph while paired t-test in the upper graph (indicated with stars). * $p < 0.05$, ** $p < 0.01$. This figure was reused from Tang et al. (2022).

Potential solution

There may be several possibilities for this problem. Firstly, the cell viability of ADSCs decreases after multiple passages. It is recommended to avoid using ADSCs after 5 passages. Secondly, the time for cell adhesion in step 20 is inappropriate. The nutrients in the first 5 μL of cell suspension added to the dish are not sufficient to support the long-term survival of the cells. Long incubation may lead to depletion of nutrients or drying up of fluids. On the contrary, short incubation may not be enough for the suspending cells to adhere to the bottom but be washed away when adding more culture medium in step 21. Therefore, it is necessary to check the waiting time accordingly.

Problem 2

The cells deteriorate during photoactivation experiments (steps 25–31).

Potential solution

If the cells deteriorate within a short time after photoactivation (within minutes), check the laser power and use some simple assays to examine photodamage. Consider reducing the power of the femtosecond laser first.

Long exposure (> 3 h) to a low-temperature environment (below 37°C) also makes cells deteriorate. Experientially, cells can maintain well at room temperature (25°C) for around 3 h. Check if the plating density of cells is appropriate and improve the operator's proficiency. If an individual experiment lasts over 3 h, please set an incubation system on the microscope stage to maintain cell viability.

Problem 3

The femtosecond laser cannot be detected at the specimen (step 22).

Potential solution

Check if the femtosecond laser at the near-infrared band is coupled into the microscope successfully. The dichroic mirrors in the optical system should match the confocal microscopy and laser penetration. Check if the automatic shutters inside the microscope are open during the

measurement. Finally, check if the power meter works for the femtosecond laser (1030 nm in this protocol) and get them corrected.

Problem 4

The proportion of differentiated ADSCs is low (steps 33 and 34).

Potential solution

The low power of the femtosecond laser may lead to low differentiation efficiency. If the ADSCs in the dish are not totally activated, the differentiation efficiency is also affected since the proliferation of differentiated cells is quite slow but the ADSCs proliferate fast along time. Be sure to activate at least 80% of the ADSCs.

Our previous study (Tang et al., 2022) showed that Ca^{2+} plays a dispensable role in stem cell differentiation by this method. Try to locate the femtosecond laser focus in ER to excite significant Ca^{2+} release of cells. (Before experiments, the ER region in bright-field microscopy of cells can be tested by fluorescent indicators of ER and colocalization of ER in the fluorescent- and bright-field microscopy). It is recommended to test the Ca^{2+} release in cells by photoactivation under different parameters of the femtosecond laser before formal experiments. Experientially, the Ca^{2+} release is significant after photoactivation. In contrast, if the femtosecond laser is not collimated, or the laser focus falls outside of the cells, the Ca^{2+} response to photoactivation becomes quite weak.

Problem 5

When the mouse cerebellum was re-observed 24 h after *in vivo* photoactivation, the *in vivo* microscopy of neurons becomes blurred (step 48).

Potential solution

Check if any bleeding or inflammation on the surface and beneath the skull. If the bleeding/inflammation is not serious, the skull can be cleaned and ground as in steps 38–39 and continue the experiment. The cerebellum can be observed by either confocal or multiphoton microscopy. Use any of it to get the optimal microscopy. If clear images of neurons cannot be acquired, it is recommended to take more careful and strict comprehensive prevention of inflammation before experiments on the first day.

RESOURCE AVAILABILITY

Lead contact

Further information and requests for resources and reagents should be directed to and will be fulfilled by the lead contact, Hao He (haohe@sjtu.edu.cn).

Materials availability

This study did not generate new unique reagents.

Data and code availability

This study did not generate any datasets or code.

ACKNOWLEDGMENTS

We thank Weiqiang Gao for the gift of the animal model: Math1-GFP; Dcx-DsRed double reporter mouse model. The work was supported by the National Natural Science Foundation of China (NSFC 62022056 and 92054105) and Science and Technology Commission of Shanghai Municipality 22ZR1430000.

AUTHOR CONTRIBUTIONS

H.H. conceived the study and led the project. W.T. performed the *in vitro* experiments and prepared the figures. H.W. performed the *in vivo* experiments. W.T. drafted the manuscript. All authors critically reviewed and revised the manuscript.

DECLARATION OF INTERESTS

The authors declare no competing interests.

REFERENCES

Burridge, P.W., Matsa, E., Shukla, P., Lin, Z.C., Churko, J.M., Ebert, A.D., Lan, F., Diecke, S., Huber, B., Mordwinkin, N.M., et al. (2014). Chemically defined generation of human cardiomyocytes. Nat. Methods *11*, 855–860. https://doi.org/10.1038/nmeth.2999.

Camp, J.G., Wollny, D., and Treutlein, B. (2018). Single-cell genomics to guide human stem cell and tissue engineering. Nat. Methods *15*, 661–667. https://doi.org/10.1038/s41592-018-0113-0.

Chaudhuri, O., Gu, L., Klumpers, D., Darnell, M., Bencherif, S.A., Weaver, J.C., Huebsch, N., Lee, H.p., Lippens, E., Duda, G.N., and Mooney, D.J. (2016). Hydrogels with tunable stress relaxation regulate stem cell fate and activity. Nat. Mater. *15*, 326–334. https://doi.org/10.1038/nmat4489.

von Erlach, T.C., Bertazzo, S., Wozniak, M.A., Horejs, C.-M., Maynard, S.A., Attwood, S., Robinson, B.K., Autefage, H., Kallepitis, C., del Río Hernández, A., et al. (2018). Cell-geometry-dependent changes in plasma membrane order direct stem cell signalling and fate. Nat. Mater. *17*, 237–242. https://doi.org/10.1038/s41563-017-0014-0.

Estes, B.T., Diekman, B.O., Gimble, J.M., and Guilak, F. (2010). Isolation of adipose-derived stem cells and their induction to a chondrogenic phenotype. Nat. Protoc. *5*, 1294–1311. https://doi.org/10.1038/nprot.2010.81.

Lee, A.S., Tang, C., Rao, M.S., Weissman, I.L., and Wu, J.C. (2013). Tumorigenicity as a clinical hurdle for pluripotent stem cell therapies. Nat. Med. *19*, 998–1004. https://doi.org/10.1038/nm.3267.

Lumpkin, E.A., Collisson, T., Parab, P., Omer-Abdalla, A., Haeberle, H., Chen, P., Doetzlhofer, A., White, P., Groves, A., Segil, N., and Johnson, J.E. (2003). Math1-driven GFP expression in the developing nervous system of transgenic mice. Gene Expr. Patterns *3*, 389–395. https://doi.org/10.1016/S1567-133X(03)00089-9.

Marker, D.F., Tremblay, M.-E., Lu, S.-M., Majewska, A.K., and Gelbard, H.A. (2010). A thin-skull window technique for chronic two-photon *in vivo* imaging of murine microglia in models of neuroinflammation. J. Vis. Exp.e2059. https://doi.org/10.3791/2059.

Muffat, J., Li, Y., Yuan, B., Mitalipova, M., Omer, A., Corcoran, S., Bakiasi, G., Tsai, L.-H., Aubourg, P., Ransohoff, R.M., and Jaenisch, R. (2016). Efficient derivation of microglia-like cells from human pluripotent stem cells. Nat. Med. *22*, 1358–1367. https://doi.org/10.1038/nm.4189.

Tang, W., Wang, H., Zhao, X., Liu, S., Kong, S.K., Ho, A., Chen, T., Feng, H., and He, H. (2022). Stem cell differentiation with consistent lineage commitment induced by a flash of ultrafast-laser activation *in vitro* and *in vivo*. Cell Rep. *38*, 110486. https://doi.org/10.1016/j.celrep.2022.110486.

Vining, K.H., and Mooney, D.J. (2017). Mechanical forces direct stem cell behaviour in development and regeneration. Nat. Rev. Mol. Cell Biol. *18*, 728–742. https://doi.org/10.1038/nrm.2017.108.

Yang, R., Wang, M., Wang, J., Huang, X., Yang, R., and Gao, W.-Q. (2015). Cell division mode change mediates the regulation of cerebellar granule neurogenesis controlled by the sonic hedgehog signaling. Stem Cell Rep. *5*, 816–828. https://doi.org/10.1016/j.stemcr.2015.09.019.

Yu, X., and Zuo, Y. (2014). Two-photon in vivo imaging of dendritic spines in the mouse cortex using a thinned-skull preparation. J. Vis. Exp, e51520. https://doi.org/10.3791/51520.